Physics Letters A 375 (2011) 2274–2277

Contents lists available at ScienceDirect

Physics Letters A

www.elsevier.com/locate/pla

Properties of optical fiber based synchronous heralded single photon sources at 1.5 µm

Qiang Zhou, Wei Zhang *, Jie-rong Cheng, Yi-dong Huang, Jiang-de Peng

Tsinghua National Laboratory for Information Science and Technology, Department of Electronic Engineering, Tsinghua University, Beijing 100084, PR China

ARTICLE INFO

Article history:
Received 29 December 2010
Received in revised form 14 March 2011
Accepted 7 April 2011
Available online 10 May 2011
Communicated by P.R. Holland

Keywords:
Heralded single photon source
Spontaneous four wave-mixing

ABSTRACT

1.5 µm synchronous heralded single photon source (HSPS) is experimentally demonstrated based on spontaneously four wave-mixing in liquid nitrogen cooled dispersion shifted fiber. Experimental results show that both preparation efficiency and conditional second order correlation function $g^{(2)}(0)$ increase with pump light level. Between the two important parameters, tradeoff should be taken to obtain high quality fiber based synchronous HSPS. A HSPS with preparation efficiency of $> 60\%$ and $g^{(2)}(0) < 0.06$ is achieved, multi-photon probability of which is reduced by a factor of > 16 compared with the Poissonian light sources. Experimental results show a great potential of the fiber based synchronous HSPS for quantum information applications.

1. Introduction

Reliable single photon sources at 1.5 µm are key elements for quantum information science [1–4]. As a traditional way, weak laser pulse sources are employed as approximate single photon sources. According to the Poissonian photon statistics property of the laser light [5], an approximate single photon source cannot achieve a high one-photon probability while its multi-photon probability is very low. As a result, security distance of the quantum cryptography system based on it is limited [6]. Recently, the decoy state protocol has been developed, enhancing the security of quantum cryptography system [7–9]. However, single photon source with high efficiency and low multi-photon events is still a bottleneck to achieve long distance security communication. An ideal single photon source based on single quantum emitter such as single atom, single quantum dot and single nitrogen-vacancy center in diamond [10], can deterministically emit one and only one photon at a time, allowing for dramatic increase of the security distance of the quantum cryptography system. However, the performance of ideal single photon source highly depends on the property of material and the photon collection technology. Although optical micro-cavities are employed to enhance the spontaneously emission efficiency of the single quantum emitter utilizing Purcell effect, and to improve the photon collection efficiency through controlling the mode property of the cavity, the total efficiency of such devices needs a further improvement for practical application. Recently, HSPS based on generation of correlated photon pair (CPP) has attracted more and more attentions. In HSPS, one photon of the photon pair is detected, and then an electrical signal is provided as the heralding signal for the appearance of the other photon. The contemporary way to realize HSPS is through spontaneous parametric down-conversion process in bulk crystal, periodically poled crystal waveguide and atomic cascades [11–14]. However, techniques still need improving for this kind of HSPS, such as collecting the photon into a single-mode fiber, adjusting and stabilizing the experimental setup [15]. More recently, CPPs generated in dispersion shifted fiber (DSF) and micro-structured fiber, with high spectral brightness and single spatial mode over broad wavelength range, have been demonstrated through spontaneous four wave-mixing (SFWM) processes [16–18]. But the quality of the generated CPP is deteriorated by noise photons from spontaneous Raman scattering (SpRS) processes in these fibers. Two methods are developed to improve the quality of CPP. One is fiber cooling technique through submerging the fiber in liquid nitrogen or liquid helium [19,20]. The other is using micro-structured fiber with special dispersion property, in which large frequency spanned CPPs are generated [21,22]. The large frequency spanned CPPs are located at the frequency range far away from the first order SpRS, which results in high quality CPPs generation and provides a way to realize high performance HSPSs [23]. However, this scheme highly relies on the dispersion characteristics of the fiber available, requires tunable pump light at 800 nm band or 1.0 µm band and needs optical components operating in a very wide frequency range.

In this Letter, a 1.5 µm synchronous HSPS is realized based on commercial fiber components and DSF with fiber cooling technique. Compared with the scheme of HSPS based on the large frequency spanned CPP generation, our scheme can utilize the well

* Corresponding author.
E-mail addresses: q-zhou06@mails.tsinghua.edu.cn (Q. Zhou), zwei@tsinghua.edu.cn (W. Zhang).

doi:10.1016/j.physleta.2011.04.044

developed technology of optical fiber communication system sufficiently.

2. Experiment of correlated photon pair generation and synchronous heralded single photon source characterization

The experimental setups for generating CPP and characterizing the synchronous HSPS are shown in Fig. 1. The CPP generating and characterizing parts are shown in Fig. 1(a) and (b) respectively. The pulsed pump is generated by a passive mode-locked fiber laser. The central wavelength of the pump light λ_p is 1552.75 nm, with a pulse width of several tens of pico-seconds (estimated by its spectral width) and 1 MHz repetition rate. A side-band rejection of 115 dB for pump light is achieved ensuring the efficient detection of the generated CPPs. A variable optical attenuator (VOA) and a 50/50 fiber coupler with a power meter (PM) are used to control and monitor the pump power level. When pump pulses pass through 500 m DSF ($\lambda_0 = 1549$ nm, fabricated by Yangtze Co., Ltd.), CPPs are generated through SFWM processes. The DSF is submerged in liquid nitrogen (77 K) to suppress the generation of SpRS photon. The output of the DSF is directed into a filtering and splitting system (in Fig. 1(b)) based on a 100 GHz/40-channel arrayed waveguide grating (AWG, Scion Photonics Inc.), two fiber Bragg gratings (FBGs), and two tunable optical band-pass filters (TOBFs). Total pump isolation is much greater than 110 dB at either signal or idler wavelength, which guarantees the reliable detection of the generated CPPs. Three InGaAs/InP avalanche photodiode-based single photon detectors (SPDs, Id Quantique, id201) are used to detect the generated CPPs and heralded single photon. All SPDs are operated under Geiger mode with detection window of 2.5 ns and detection efficiency of $\xi_1 = 16.42\%$, $\xi_2 = 21.83\%$ and $\xi_3 = 22.56\%$ for SPD1, SPD2 and SPD3, respectively. All photon counts are measured with a 30-second counting time and averaged after 5-time measurement.

First, the generation of CPPs in 500 m DSF submerged in liquid nitrogen is demonstrated. In the experiment four photon count rates are measured (i.e. the single side counts rates of signal and idler side photon, coincidence and accidental coincidence count rates) under different pump power levels. And the generation rates of correlated photon pair and SpRS photon can be obtained through the method in Refs. [24,25]. Fig. 2(a) is the results of the obtained generation rates of photon. The squares and circles are the generation rates of CPP R_c and SpRS photon on signal side R_{s-R}, respectively; the solid and the dashed line are the fitting curve of $R_c = 837.2P_{av}^2$ and $R_{s-R} = 2.1P_{av}$, respectively, where P_{av} is the average power of the pump light. Though the result indicates that SFWM processes dominate the photon generation and the SpRS processes are suppressed by fiber cooling technique, R_{s-R} is comparable with R_c while the pump power level is low. The frequency correlation property of the generated CPPs is demonstrated by observing the ratios between coincidence count (N_{co}) and accidental coincidence count (N_{ac}) under a fixed idler side wavelength λ_i of 1550.35 nm and different signal side wavelengths. Fig. 2(b) shows the experimental results. An averaged ratio of 16.46 is achieved at λ_s of 1555.15 nm while the averaged ratios are about 1 at other signal side wavelengths, showing the strong frequency correlation property of the generated CPPs.

To realize a synchronous HSPS, the generated CPPs are directed into a modified filtering and splitting system as shown in Fig. 1(c), in which λ_i and λ_s are set at 1550.35 nm and 1555.15 nm, respectively. In order to improve collection efficiency of the heralded single photon (idler photons in the experiment), the FBG2 in the idler side is removed, since the heralding signal (generated by the detection of the signal photon) can pick the idler photon out, according to the frequency correlation property of the CPPs. A loss of $\alpha = 2.6$ dB on heralded photon side is achieved in the experiment, while a loss of 3.4 dB on heralding photon side. In the experiment, the measured preparation efficiency η_p (i.e. probability of output of idler photon under a heralding signal given by the detection of the signal photon) of the synchronous HSPS is obtained by $N_2/(\xi_2 N_1)$, where N_1 is the photon counts of SPD1, N_2 is the photon counts of SPD2 trigger by the output of SPD1, and ξ_2 is the detection efficiency of SPD2.

The preparation efficiency η_p is determined by the loss of the filtering and splitting system on the heralded photon side, the multi-photon events in one heralded photon wave-packet and the noise photon on the heralding photon side (such as the SpRS photon, the residual pump photon and the dark counts of SPD1, among which the residual pump photon and the dark counts of SPD1 can be neglected). The effect of the loss on the heralded photon side and the multi-photon events can be expressed by η_{p0} shown in Eq. (1), which provides the up-limit of the synchronous HSPS preparation efficiency

$$\eta_{p0} = 10^{-\frac{\alpha}{10}} \times \frac{\sum_{n=1}^{+\infty} p(n)(1-(1-\xi_2)^n)}{\xi_2} \tag{1}$$

where $p(n)$ $(n = 1, 2, \ldots)$ is the probability of n photons in one heralded photon wave-packet when a heralding signal is given.

On the other hand, although the SpRS photon can be suppressed by fiber cooling, it is still comparable with the CPPs when the pump light level is very low. On this condition, η_p is determined by

$$\eta_p = \eta_{p0}/(1 + R_{s-R}/R_c) \tag{2}$$

where R_c and R_{s-R} can be obtained through the result in Fig. 1(a), respectively.

The result of preparation efficiency is shown in Fig. 3(a). The solid line in Fig. 3(a) is the calculated η_{p0}, the minimum of which is 54.95% determined by the loss of 2.6 dB on heralded photon side. Due to the increase of the multi-photon events, η_{p0} increases with R_c. The squares in Fig. 3(a) are the experimental results of preparation efficiencies under different R_c. It is worth noting that η_p is much less than η_{p0} while R_c is small, owing to the influence of the SpRS photon on the heralding side. The dashed line in Fig. 3(a) is the fitting curve of η_p considering the influence of SpRS photon on the heralding side through Eq. (2). It can be seen that η_p increases with R_c and becomes close to η_{p0}, thanks to the decrease of R_{s-R}/R_c.

Then, $g^{(2)}(0)$ of the heralded photons is measured through a Hanbury-Brown and Twiss (HBT) setup (shown in Fig. 1(d)) [26]. The two output ports of the HBT setup are detected by SPD2 and SPD3, respectively, which are triggered by the output of SPD1. Conditional on the detection of the heralding photon, $g^{(2)}(0)$ of the heralded photon is calculated by [27,28]

$$g^{(2)}(0) = \frac{p_{23}(2)}{p_2(1)p_3(1)} \approx \frac{2p(2)}{p^2(1)} \tag{3}$$

where $p_2(1) \approx \xi_2 p(1)/2$ and $p_3(1) \approx \xi_3 p(1)/2$ represent the probability of detecting one photon at the heralded side by detector SPD2 and SPD3, respectively. $p_{23}(2) \approx \xi_2\xi_3 p(2)/2$ represents the joint probability of simultaneously detecting one photon by SPD2 and SPD3. In the experiment, $g^{(2)}(0)$ under different R_c is measured and given in Fig. 3(b). It shows that $g^{(2)}(0)$ also increases with R_c due to the increase of the multi-photon probability.

For a perfect single photon source and SPDs, $g^{(2)}(0)$ equals zero. For any sources with non-zero probability of multi-photon event, $g^{(2)}(0)$ is greater than zero. $0 < g^{(2)}(0) < 1$ indicates the non-classical nature of the photon source. In the experiment, $g^{(2)}(0) < 0.06$ is achieved and demonstrates the non-classical nature of our synchronous HSPS while the preparation efficiency is $> 60\%$. Compared with the approximate single photon sources, the

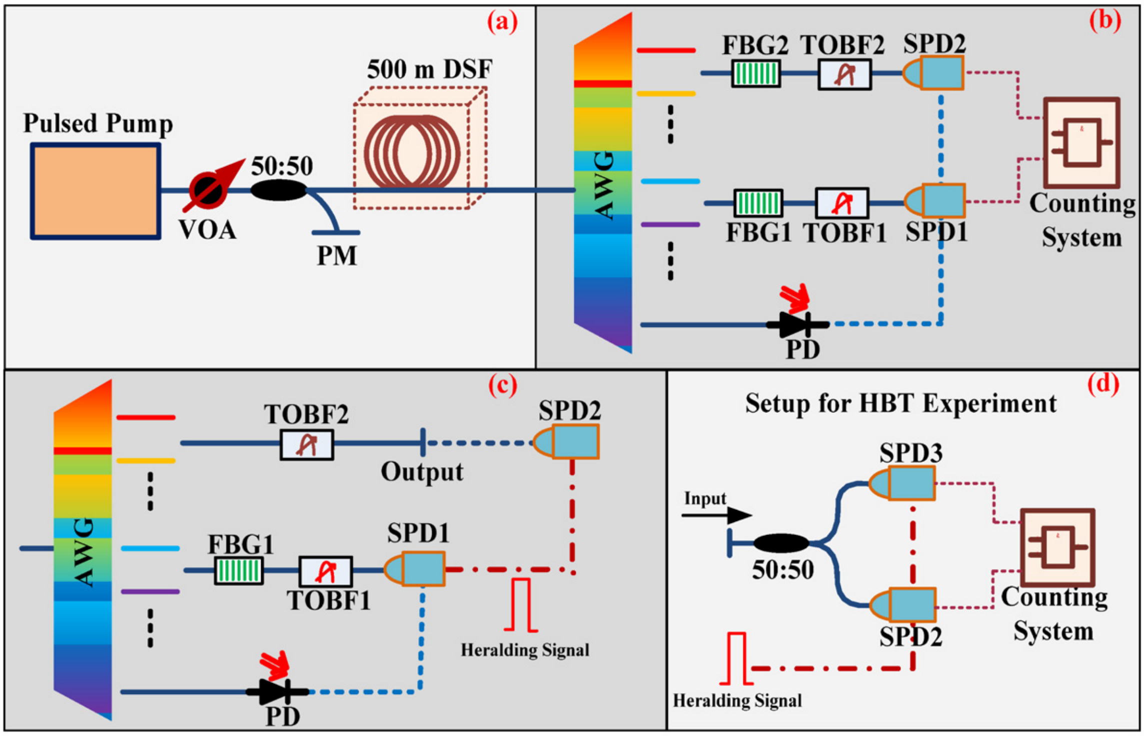

Fig. 1. Experimental setup. (a) is the correlated photon pair generation parts. (b) is the correlated photon pair characterization parts. (c) is the modified heralded single photon source parts. (d) is the Hanbury-Brown and Twiss (HBT) setup. VOA: variable optical attenuator; PM: power meter; DSF: dispersion shifted fiber; AWG: arrayed waveguide grating; FBG: fiber Bragg grating; TOBF: tunable optical band-pass filter; SPD: single photon detector; PD: photo-detector.

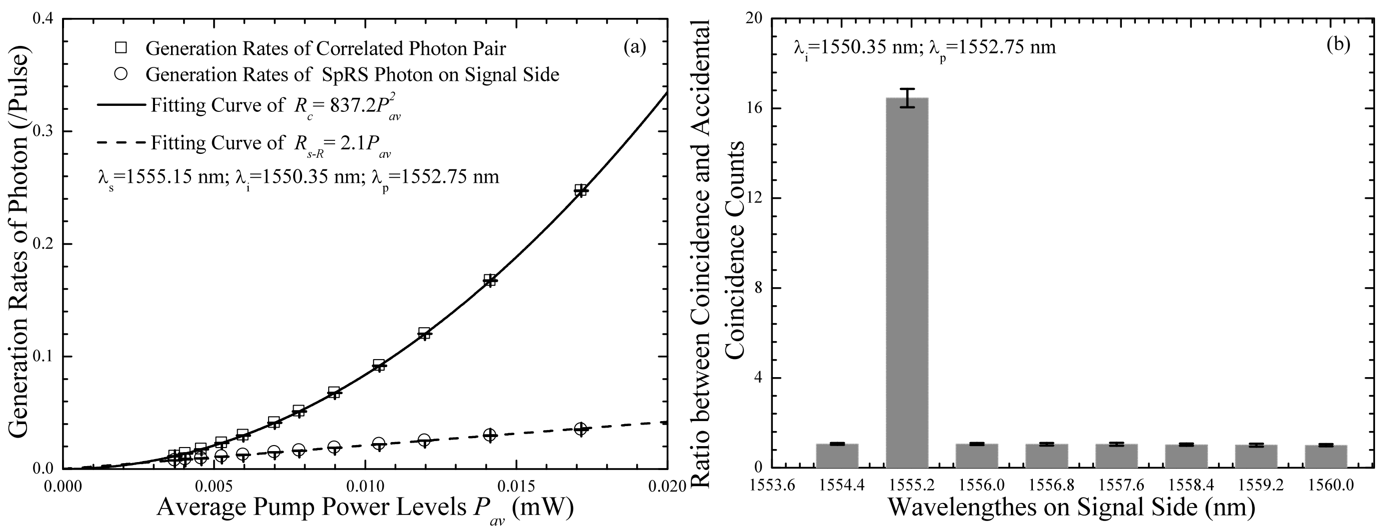

Fig. 2. Experimental result of CPP generation in 500 m DSF. (a) is the obtained generation rates of photon under different pump power level P_{av}, the squares and circles are the R_c and R_{s-R}, respectively; the solid and the dashed line are the fitting curve of $R_c = 837.2P_{av}^2$ and $R_{s-R} = 2.1P_{av}$, respectively. (b) is the frequency correlation properties of the generated correlated photon pairs with $\lambda_i = 1550.35$ nm and $\lambda_p = 1552.75$ nm.

multi-photon probability of the synchronous HSPS is reduced by a factor of more than 16. Since both the preparation efficiency and $g^{(2)}(0)$ increase with the R_c, tradeoff between them should be taken carefully for a high quality fiber based synchronous HSPS.

3. Conclusion

In this Letter, we have experimentally demonstrated and characterized a 1.5 μm synchronous HSPS based on DSF and commercial fiber components. Experimental results show that both its preparation efficiency and $g^{(2)}(0)$ increase with the pump light level. Tradeoff between these two important parameters should be taken for the fiber based synchronous HSPS. A HSPS with a preparation efficiency of $> 60\%$ and $g^{(2)}(0) < 0.06$ is achieved in the experiment, which shows the great potential of the fiber based synchronous HSPS for quantum information applications.

Acknowledgements

This work is supported in part by National Natural Science Foundation of China under Grant No. 60777032, 973 Programs of China under Contract Nos. 2010CB327600 and 2011CBA00303, Tsinghua University Initiative Scientific Research Program under Contract No. 2010THZ0, Science Foundation of Beijing under Grant No.

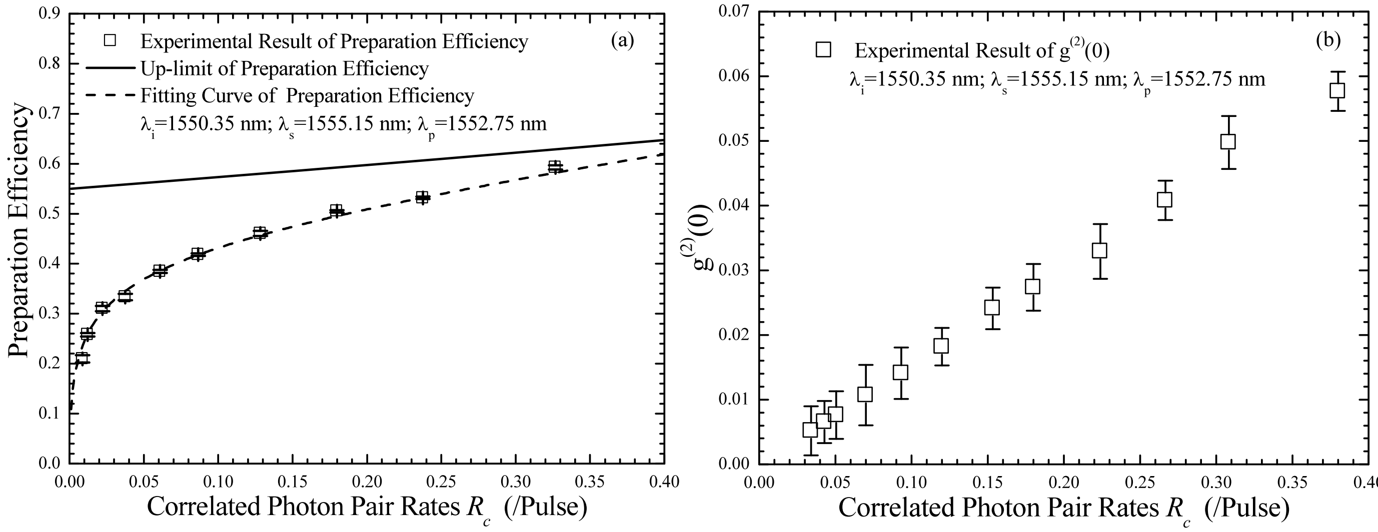

Fig. 3. Preparation efficiency and conditional second-order correlation function $g^{(2)}(0)$ of the synchronous HSPS under different R_c. (a) is the preparation efficiency under different R_c. The solid line is the up-limit of preparation efficiency determined by the loss on the heralded photon side of filtering and splitting system and the multi-photon events in one heralded photon wave-packet. The squares are the experimental result of the preparation efficiency under different R_c. The dashed line is the fitting curve of the preparation efficiency with the influence of SpRS photon. (b) is the experimental result of conditional second-order correlation function $g^{(2)}(0)$ under different R_c.

4102028, and Basic Research Foundation of Tsinghua National Laboratory for Information Science and Technology (TNList).

References

[1] N. Gisin, G. Ribordy, W. Tittel, H. Zbinden, Rev. Mod. Phys. 74 (2002) 145.
[2] J.L. O'Brien, A. Furusawa, J.A. Vuckovic, Nature Photon. 3 (2009) 687.
[3] P. Kok, W.J. Munro, K. Nemoto, T.C. Ralph, J.P. Dowling, G.L. Milburn, Rev. Mod. Phys. 79 (2007) 135.
[4] Q. Wang, W. Chen, G. Xavier, M. Swillo, T. Zhang, S. Sauge, M. Tengner, Z. Han, G. Guo, A. Karlsson, Phys. Rev. Lett. 100 (2008) 090501.
[5] L. Mandel, E. Wolf, Optical Coherence and Quantum Optics, Cambridge University Press, 1995, pp. 1084–1088 (Chapter 22.4.7).
[6] N. Lütkenhaus, Phys. Rev. A 61 (2000) 052304.
[7] W.Y. Hwang, Phys. Rev. Lett. 91 (2003) 057901.
[8] X.B. Wang, Phys. Rev. Lett. 94 (2005) 230503.
[9] H.K. Lo, X. Ma, K. Chen, Phys. Rev. Lett. 94 (2005) 230504.
[10] A. Kuhn, D. Ljunggren, Contemp. Phys. 4 (2010) 289.
[11] C.K. Hong, L. Mandel, Phys. Rev. Lett. 56 (1986) 58.
[12] A.B. U'Ren, C. Silberhorn, J.L. Ball, K. Banaszek, I.A. Walmsley, Phys. Rev. A 72 (2005) 021802(R).
[13] P. Grangier, G. Roger, A. Aspect, Europhys. Lett. 1 (1986) 173.
[14] O. Alibart, D.B. Ostrowsky, P. Baldi, Opt. Lett. 12 (2005) 1539.
[15] A. Fedrizzi, T. Herbst, A. Poppe, T. Jennewein, A. Zeilinger, Opt. Express 15 (2007) 15377.
[16] M. Fiorentino, P.L. Voss, J.E. Sharping, P. Kumar, IEEE Photon. Technol. Lett. 14 (2002) 983.
[17] J. Sharping, J. Chen, X. Li, P. Kumar, R.S. Windeler, Opt. Express 12 (2004) 3086.
[18] Q. Zhou, W. Zhang, J. Cheng, Y. Huang, J. Peng, Opt. Lett. 34 (2009) 2706.
[19] H. Takesue, K. Inoue, Opt. Express 13 (2005) 7832.
[20] S.D. Dyer, B. Baek, S.W. Nam, Opt. Express 17 (2009) 10290.
[21] C. Soller, B. Brecht, P.J. Mosley, L.Y. Zang, A. Podlipensky, N.Y. Joly, P.St.J. Russell, C. Silberhorn, Phys. Rev. A 81 (2010) 031801.
[22] J.A. Slater, J. Corbeil, S. Virally, F. Bussières, A. Kudlinski, G. Bouwmans, S. Lacroix, N. Godbout, W. Tittel, Opt. Lett. 35 (2010) 499.
[23] E.A. Goldschmidt, M.D. Eisaman, J. Fan, S.V. Polyakov, A. Migdal, Phys. Rev. A 78 (2008) 013844.
[24] W. Zhang, Q. Zhou, J.R. Cheng, Y.D. Huang, J.D. Peng, Eur. Phys. J. D 59 (2010) 309.
[25] Q. Zhou, W. Zhang, J. Cheng, Y. Huang, J. Peng, Opt. Express 34 (2010) 17114.
[26] R. Hanbury Brown, R.Q. Twiss, Nature 178 (1956) 1046.
[27] R.J. Glauber, Phys. Rev. 131 (1963) 1766.
[28] R.J. Glauber, Phys. Rev. 130 (1963) 2529.